Supporting information

Improved Storage Stability of Conjugated Polymer Solutions with a Versatile Non-Halogenated Solvent for Organic Solar Cells

Ying Chen, Zhenhan Zhao, Ke Zhou, Ncedo Jili, Genene Tessema Mola, Hong Zheng,* and Wei Ma**

Y. Chen, K. Zhou, W. Ma

State Key Laboratory for Mechanical Behavior of Materials, Xi'an Jiaotong University, Xi' an, 710049 China

msekzhou@xjtu.edu.cn (K. Zhou), msewma@xjtu.edu.cn (W. Ma)

Z. Zhao, H. Zheng

Centre of Nanomaterials for Renewable Energy, State Key Laboratory of Electrical Insulation and Power Equipment, School of Electrical Engineering, Xi'an Jiaotong University, Xi'an, 710049 China

zhenghong666@xjtu.edu.cn

N. Jili, G. T. Mola

School of Chemistry & Physics, University of KwaZulu-Natal, Pietermaritzburg Campus, Private Bag X01, Scottsville, Pietermaritzburg, 3209 South Africa

Experimental section

Materials. PM6 was purchased from Volt-Amp Optoelectronics Tech. Co., Ltd. L8-BO and BTP-ec9 were purchased from Hyper, Inc. PCE10 and PTQ10 were purchased from Organtec Ltd. PDINO was purchased from Vizuchem. 1,3-Dibromo-5-chlorobenzene (DBCL) was purchased from Tokyo Chemical Industry Co., Ltd. [1] Toluene and 1,2,4-Trimethylbenzene (TMB) were purchased from Sigma-Aldrich. All chemicals and solvents were used as received without further purification.

Device fabrication. The devices were fabricated with a structure of glass/indium tin oxide (ITO)/poly(3,4-ethylenedioxythiophene):polystyrene sulfonate (PEDOT:PSS)/donor/acceptor/PDINO/Al. The patterned ITO substrate was continuously cleaned two times by sonication in water with detergent, deionized water, acetone, and isopropanol for 30 min of each step. Then the substrate was dried with a nitrogen gun. After ultraviolet ozone treatment for 15 min, PEDOT:PSS (Heraeus Clevios PVP AI 4083) was spin-coated on the prepared ITO glasses with a thickness of about 30 nm and baked at 150℃ for 15 min in air. For PM6/L8-BO OSCs, the PM6 solutions were prepared in Toluene and TMB at concentrations of 7 mg mL^{-1}, respectively. The L8-BO solutions were prepared in Toluene at concentrations of 10 mg mL^{-1}, with additive of 80% DBCL. The PM6 solution was deposited on top of the PEDOT:PSS layer by blade-coating with the blade speed of 30 mm s^{-1} at substrate temperature of 50 ℃ to form a front layer. After that, L8-BO solutions were also blade-coated onto the surfaces of donor layers with the blade speed of 45 mm s^{-1} at substrate temperature of 50 ℃. The gap between the blade and the substrate was about 200 μm. For PM6/L8-BO:BTP-ec9 OSCs, the L8-BO:BTP-ec9 solutions (0.6:0.4) were prepared in Toluene at total concentrations of 10 mg mL^{-1} with 80% DBCL. For PTQ10/L8-BO and PCE10/L8-BO OSCs, the concentrations of donor and acceptor solutions are 7 mg mL^{-1} and 10 mg mL^{-1}. The final films were transferred to the N_2-filled glovebox with annealing heat treatment (80 ℃, 10 min). Afterwards, a thin PDINO layer (2 mg mL^{-1} in methanol, 3300 rpm for 30 s) was spin coated on the active layer. Finally, a 100 nm Al were sequentially deposited as anode below the vacuum

level of 1×10^{-4} Pa. The device active area of typical device is 0.04 cm^2.

Film thickness. The film thickness was measured by a surface profilometer (Dektak XT, Bruker). The thickness of the donor layer in the active layer film was controlled to be between 50 and 60 nm, while the acceptor layer was maintained at 45 to 55 nm. The hole transport layer and electron transport layer were approximately 25 and 10 nm, respectively. When preparing the films using blade-coating method with solutions aged for different times, the gap between blade and substrate and coating speed were adjusted to ensure that the active layers had similar thickness, thereby eliminating the influence of thickness on device efficiency.

Viscosity test. The viscosity was measured using the Ulster viscometer at room temperature by recording the time required for the liquid level to flow between two lines. The operation was repeated three times, and the average of the three times was taken as the outflow time *t* of the solution. The difference between each measured value and the average value must not exceed 0.25% of the average value. The viscosity of solution can be calculated using the equation below.

$$v = K\,t$$

Where v is the viscosity of solution, K is viscometer constant.

Device characterizations. The *J-V* characteristics were measured in the N_2 glovebox under AM 1.5 G (100 mW cm^{-2}) using an AAA solar simulator (SS-F5-3A, Enli Technology CO, Ltd.) calibrated with a stander photovoltaic cell equipped with a KG5 filter and a Keithley 2400 source meter unit. The EQE was measured by Solar Cell Spectral Response Measurement System QE-R3018 (Enli Technology CO., Ltd.). The light intensity was calibrated with a standard Si photovoltaic cell.

Details of first-principle calculation. For the analysis of interaction between PM6 and the Toluene/TMB, a PM6 unit was constructed for saving computational cost. The PM6 unit was optimized with the ωB97XD functional.[2] The 6-31G(d) basis set was used for the C, O, H, and F atoms,[3,4] whereas the Los Alamos effective core potential (ECP) LANL2DZ[5] was used for the S atoms. Then, a Toluene/TMB molecule was put near the PM6 unit and the complex was also optimized at the ωB97XD/6-31G(d)~

LANL2DZ level. For the adsorption site of the solvent molecule, we calculated four types of adsorption sites and the lowest-energy one is esteemed as the most possible adsorption model. These calculations were performed with the Gaussian16 package.[6] The interaction energy between the PM6 unit and solvent molecule was further analyzed by the energy decomposition analysis (EDA)[7] with the MULTIWFN program.[8]

The first-principles molecular dynamics (AIMD) calculations were performed with the Vienna Ab Initio Simulation Package (VASP).[9] The exchange correlation interactions were estimated by the generalized gradient approximation (GGA) with Perdew-Burke-Ernzerhof (PBE) functional[10], and the electron-ion interaction was described by projector augmented-wave (PAW) pseudopotential.[11] An energy cutoff of 500 eV was chosen for the plane wave basis. The contribution of van der Waals (vdW) interactions was considered using DFT-D2 method.[12] The structure of simplified PM6 was relaxed until the forces exerted on each atom were less than 0.01eV $Å^{-1}$. For AIMD analysis, the initial lattices constant of the two systems was a = 19.98 Å, b = 20 Å and c = 12 Å. The temperature is set at room temperature 300K and the time step was set to 1 fs with 6000 steps, resulting in a total simulation time of 6 ps in the NPT ensemble.[13]

Morphology characterizations. The UV−vis absorption spectrum was measured by a Shimadzu UV-3600 Plus Spectrophotometer. The thickness of photosensitive layer was measured using a Bruker DektakXT. Atomic force microscopy (AFM) images were scanned by Veeco INNOVA Atomic Force Microscope using a tapping mode. Transmission electron microscopy (TEM) was performed using a JEM-F200 instrument at 200 kV accelerating voltage. Photoluminescence (PL) spectra measurements were performed by the FLS1000 Fluorescence spectrometer. For each aging time, PL spectra of five PM6/L8-BO films were measured to obtain an average value. For the freeze drying TEM and AFM tests, polymer solutions were deposited onto silicon substrates for AFM and onto copper grids for TEM analysis. Subsequently, the substrate was placed into a Schlenk flask for freeze-drying. Then the polymer solution was rapidly frozen using liquid nitrogen.[14]

Grazing Incidence Wide-Angle X-ray Scattering (GIWAXS) Characterization. GIWAXS measurements were performed at beamline 7.3.3[15] at the Advanced Light Source. Samples were prepared on Si substrates using identical blend solutions as those used in devices. The 10 keV X-ray beam was incident at a grazing angle of 0.11°-0.15°, selected to maximize the scattering intensity from the samples. The scattered x-rays were detected using a Dectris Pilatus 2M photon counting detector.

Measurement of solvent polarity parameter E_T(30).[16] The Reichardt's dye was prepared with two solvents respectively to form solutions at a concentration of 3×10^{4} mol L^{-1}. Then the UV-Vis absorption spectra of Reichardt's Dye in two different solvents were measured. The electronic transition energy of the longest absorption band λ_{max} of Reichardt's Dye is used to define $E_T(30)$, which can be calculated using the following equation.

$$E_T(30) = 28591/\lambda_{max}$$

In-situ Ultraviolet-visible (UV-vis) Absorption Measurements. In-situ UV-vis absorption measurements were performed by the Filmetrics F20-EXR spectrometer using the reflection mode with the time resolution of 0.01 s. The detector collects the transmission spectra ranged from 400 to 1050 nm during coating.

In-situ Photoluminescence Spectra Measurements. In-situ Photoluminescence Spectra Measurements were performed by a laser device (MGL-III-785-300mW BH81223) using the reflection mode with the time resolution of 0.1 s. The excitation wavelength was 532 nm.

Space-charge-limited-current (SCLC) mobility measurement: The mobilities were measured by using space-charge-limited-current (SCLC) model with the hole-only device of ITO/PEDOT:PSS/active layer/MoO3/Al and electron-only device of ITO/ZnO/active layer/PDINO/Al. Hole mobility and electron mobility were obtained by fitting the current density-voltage curves and calculated by the equation below.[17]

$$J = 9\varepsilon_0\varepsilon_r\mu(V_{appl} - V_{bi} - V_s)^2/8L^3$$

Where J is current density, ε_0 is the permittivity of free space, ε_r is the relative permittivity of the material, μ is hole mobility or electron mobility, V_{appl} is the applied

voltage, V_{bi} is the buit-in voltage (0 V), V_s is the voltage drop from the substrate's series resistance and L is the thickness of film.

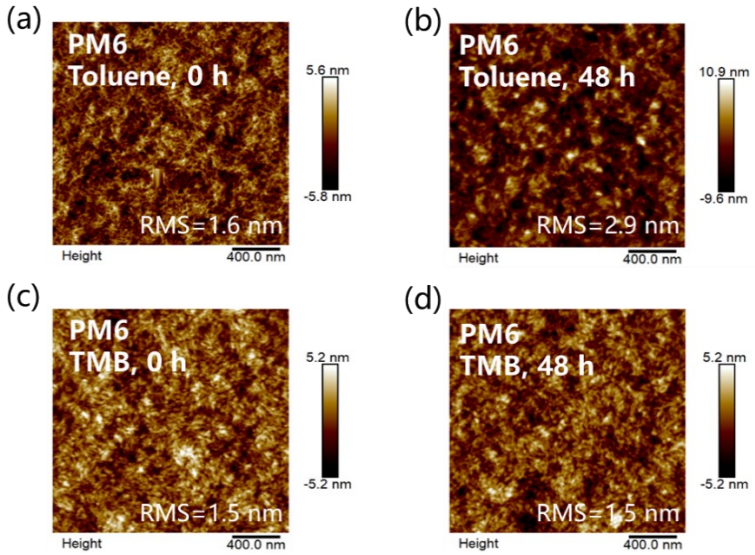

Figure S1. AFM images of PM6 films prepared by solutions that (a) (c) not be aged and (b) (d) be aged for 48 hours when using Toluene/TMB as the solvent.

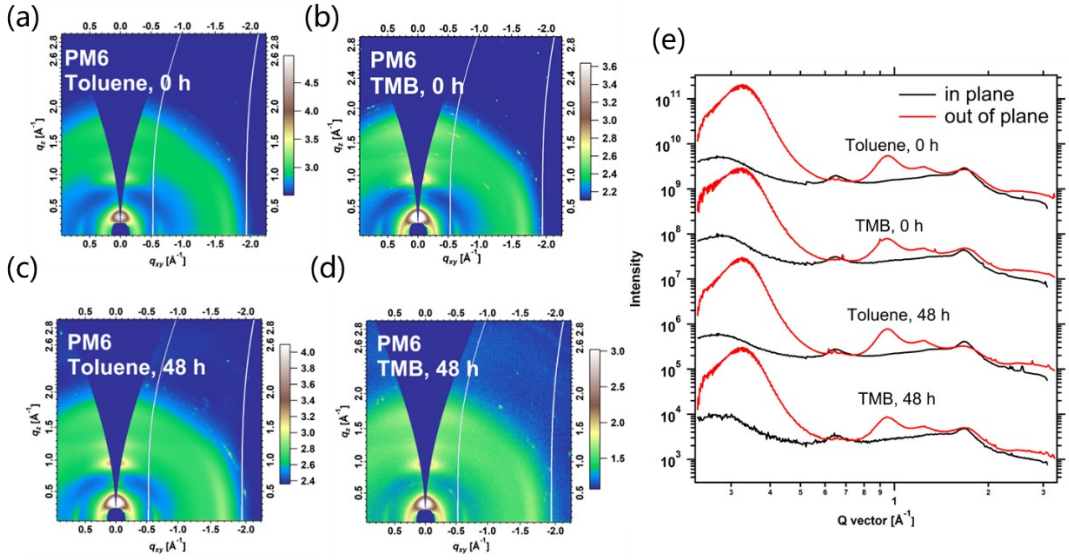

Figure S2. GIWAXS (a-d) 2D images and (e) line profiles of PM6 thin films.

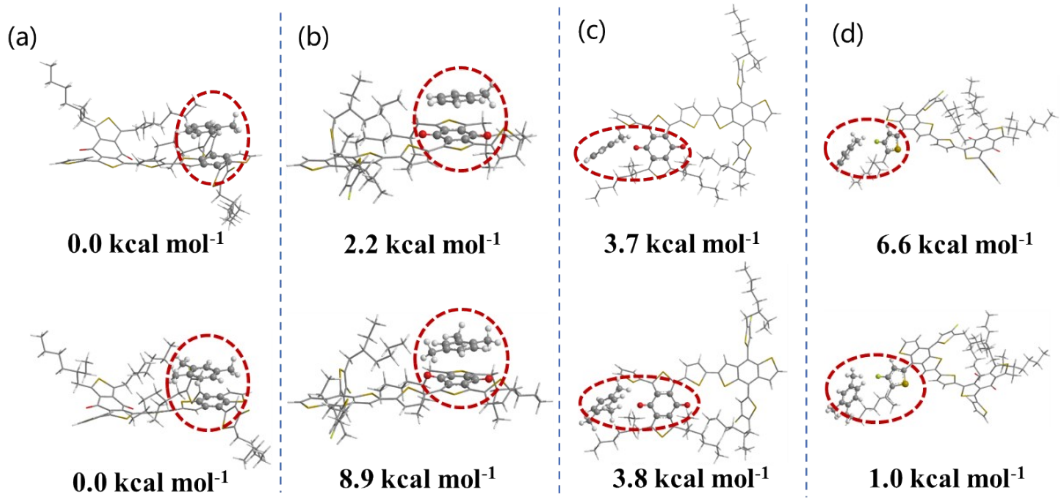

Figure S3. Schematic diagrams and relative energies of (a) the π-π stacking of carbon-carbon double bonds between the PM6 molecule and solvent molecule, (b) the π-π stacking of carbon-carbon double bonds (PM6 molecule) and carbon-sulfur double bonds (solvent molecule), (c) the hydrogen bonds between H atoms (solvent molecule) and O atoms (PM6 molecule), (d) the hydrogen bonds between H atoms (solvent molecule) and F atoms (PM6 molecule).

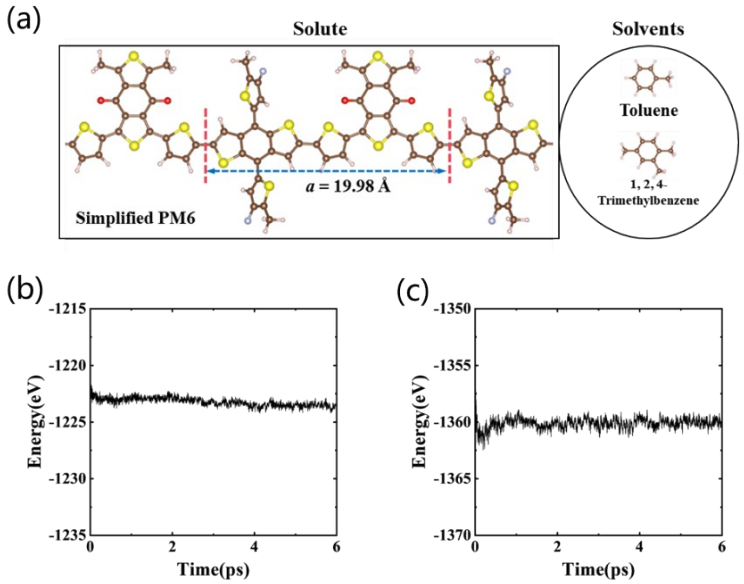

Figure S4. (a) The structures of simplified PM6 and two solvents. Fluctuations of total energy in (b) Toluene and (c) TMB during AIMD simulation.

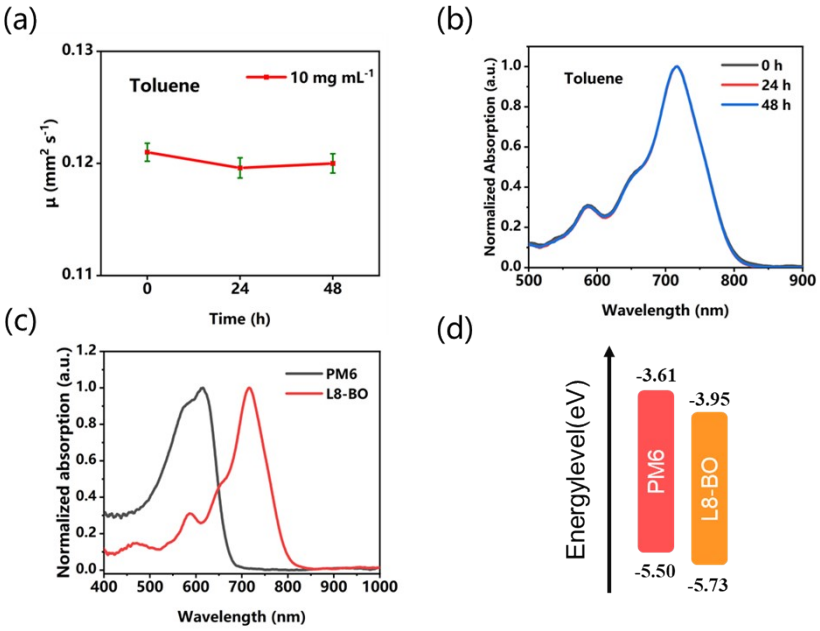

Figure S5. (a) Viscosities and (b) UV-vis absorption spectra of L8-BO solutions that be aged for different times. (c) UV-vis absorption spectra and (d) energy levels of PM6 and L8-BO.

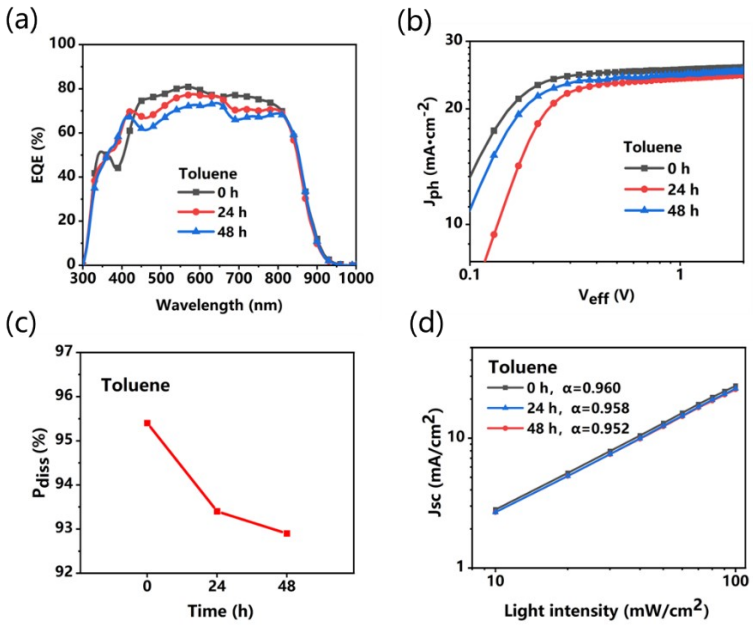

Figure S6. (a) EQE curves, (b) J_{ph}-V_{eff} curves, (c) exciton dissociation efficiency, (d) V_{OC}-Light intensity curves of PM6/L8-BO OSCs that Toluene is used as the solvent of PM6 solutions.

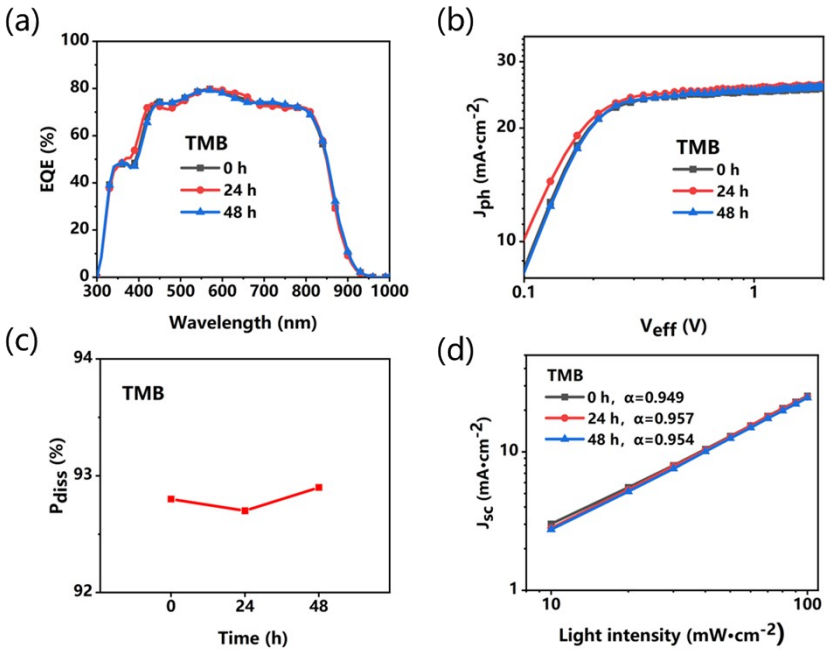

Figure S7. EQE curves, (b) J_{ph}- V_{eff} curves , (c) exciton dissociation efficiency, (d) V_{OC}-Light intensity curves of PM6/L8-BO OSCs that TMB is used as the solvent of PM6 solutions.

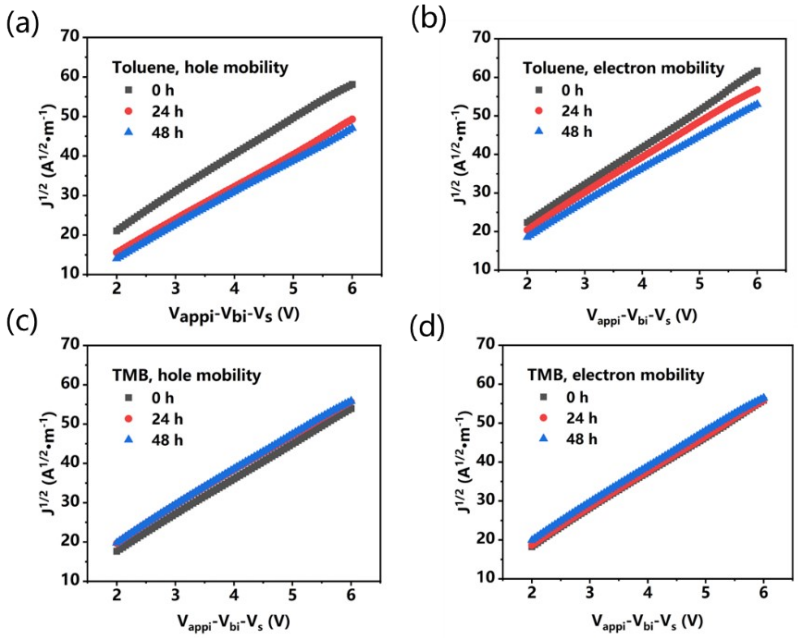

Figure S8. $J^{1/2}$-V characteristics of PM6/L8-BO OSCs when Toluene/TMB was used as the solvent of PM6 solutions.

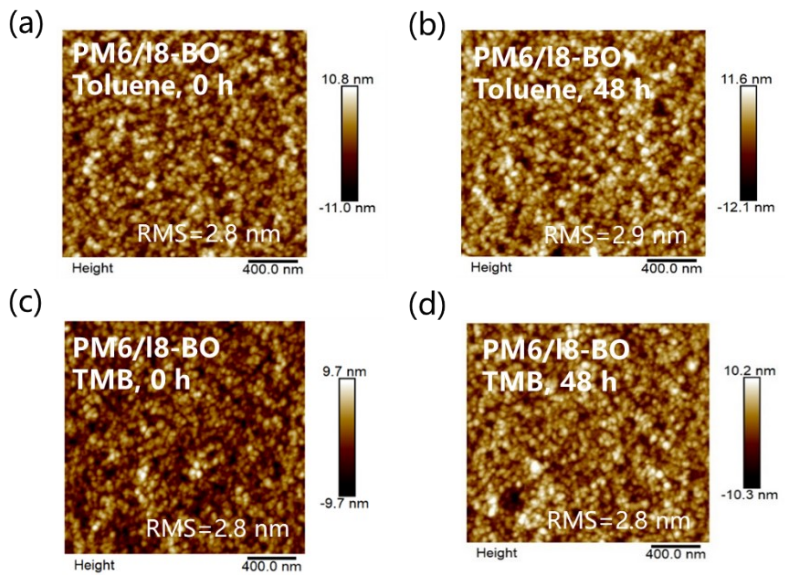

Figure S9. AFM images of PM6/L8-BO films that Toluene/TMB was used as the solvent of PM6 solutions.

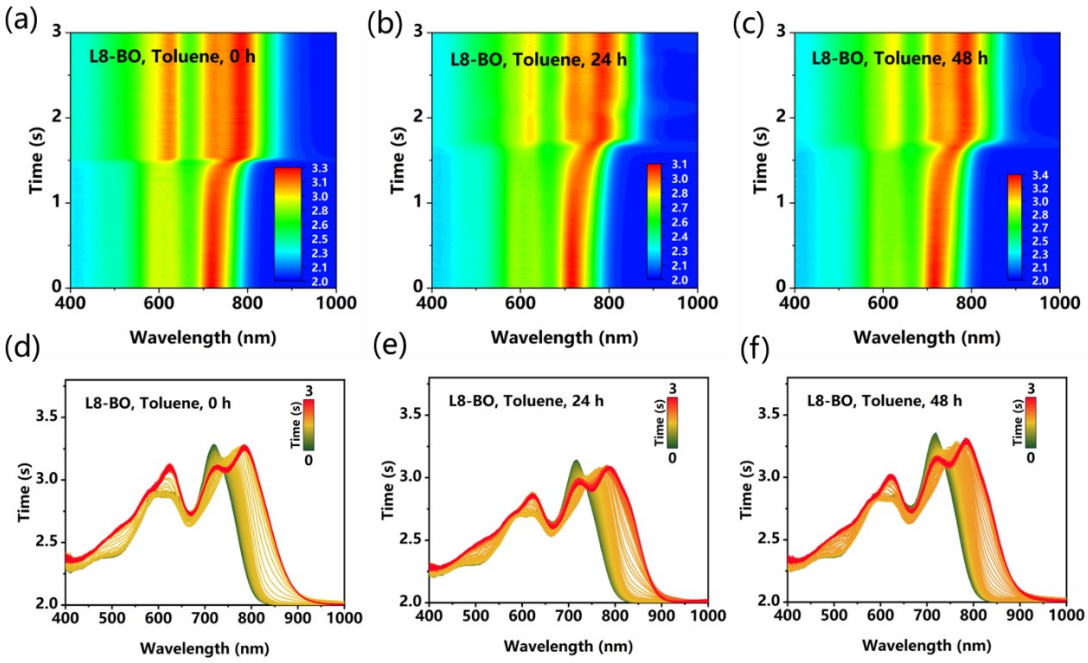

Figure S10. Contour plots and spectra of *in situ* UV of L8-BO under different aging times when Toluene was used as the solvent of PM6 solutions.

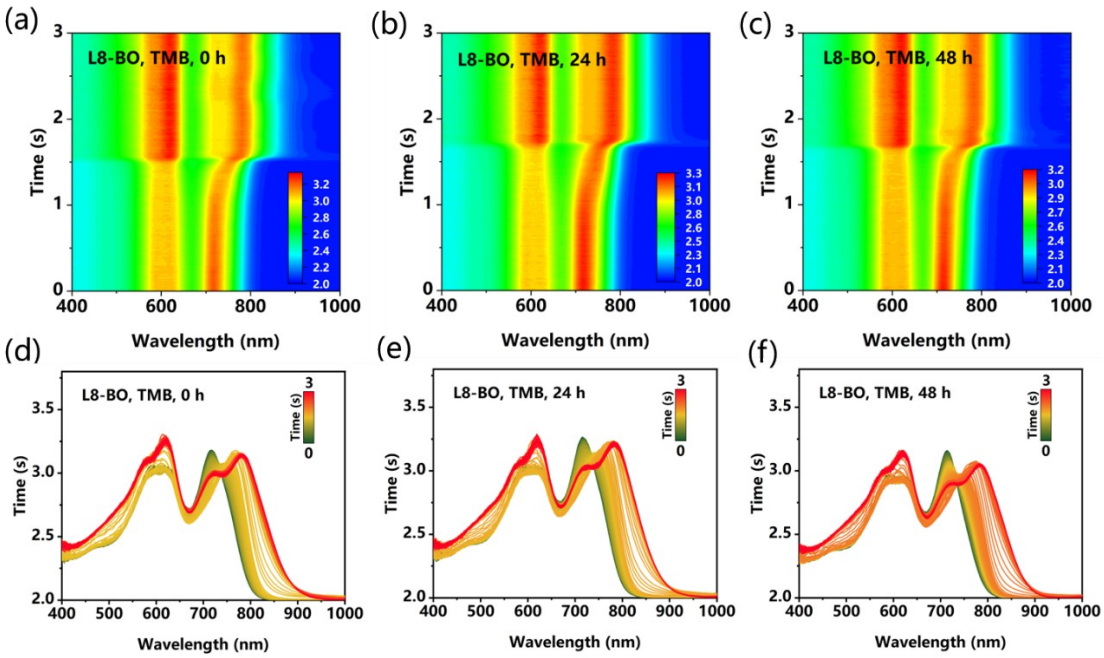

Figure S11. Contour plots and spectra of *in situ* UV of L8-BO under different aging times when TMB was used as the solvent of PM6 solutions.

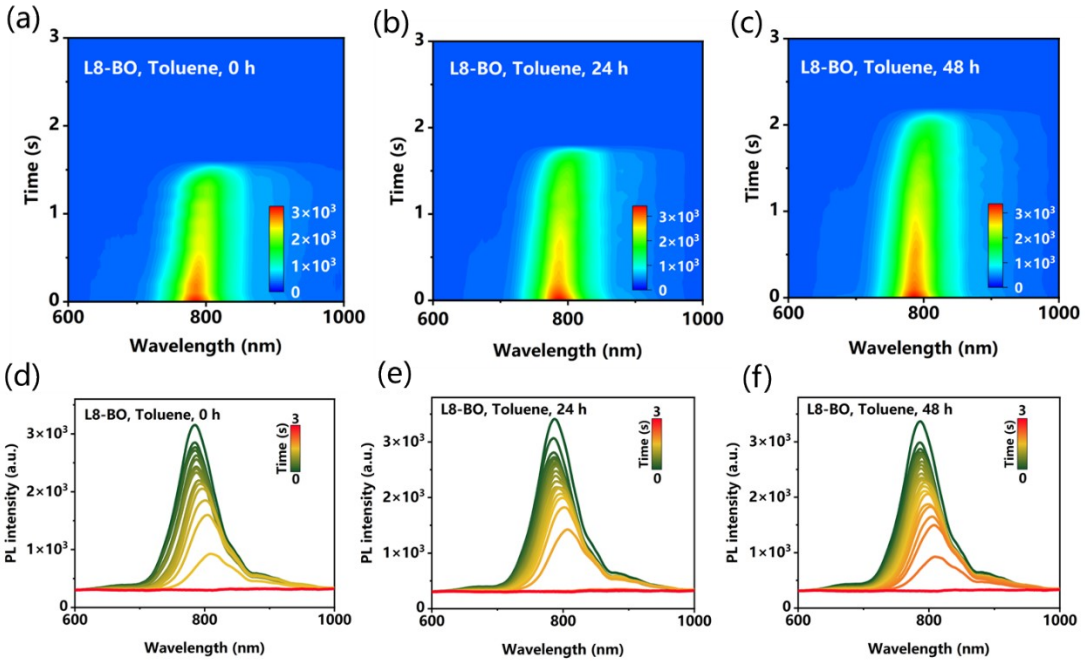

Figure S12. Contour plots and spectra of *in situ* PL of L8-BO under different aging times when Toluene was used as the solvent of PM6 solutions.

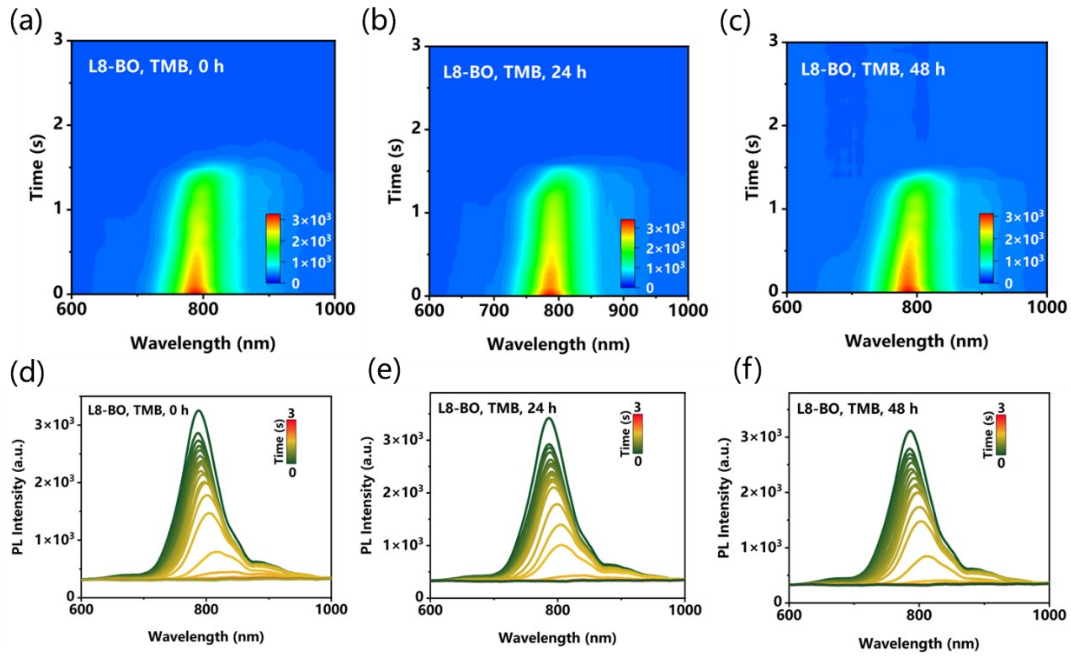

Figure S13. Contour plots and spectra of *in situ* PL of L8-BO under different aging times when TMB was used as the solvent of PM6 solutions.

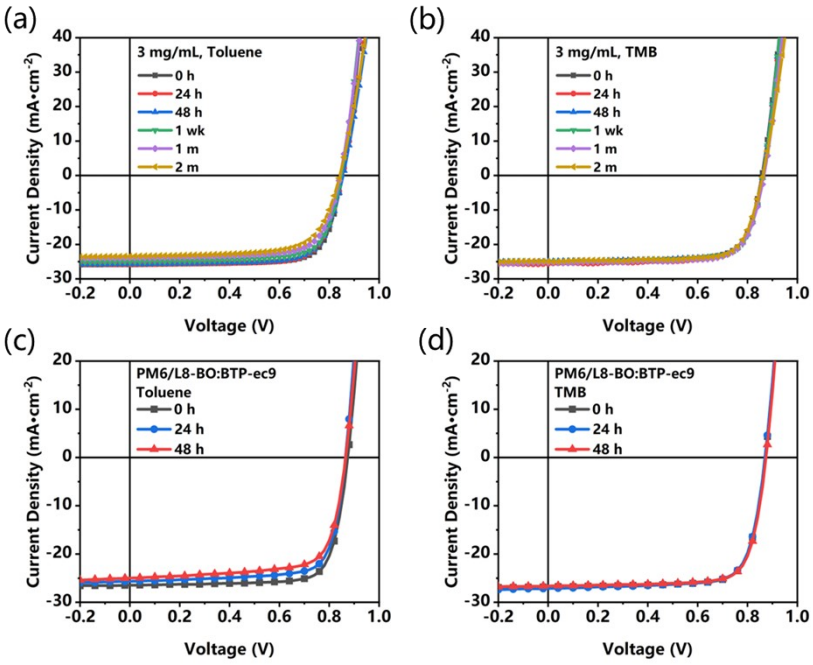

Figure S14. *J-V* curves of PM6/L8-BO OSCs using 3mg mL^{-1} PM6 solutions and PM6/L8-BO:BTP-ec9 OSCs with different solvents and aging times.

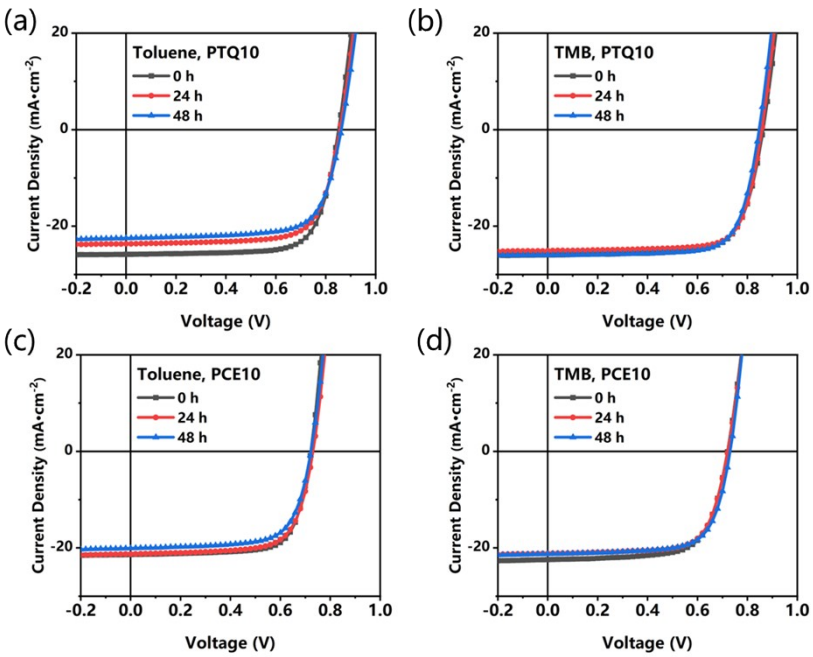

Figure S15. *J-V* curves of PTQ10/L8-BO and PCE10/L8-BO OSCs using Toluene/TMB as the solvent of PM6 solutions with different aging times.

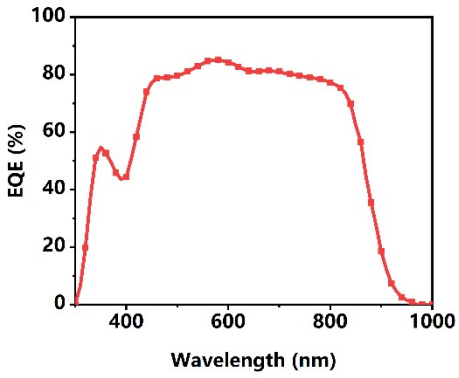

Figure S16. EQE curve of the champion cell.

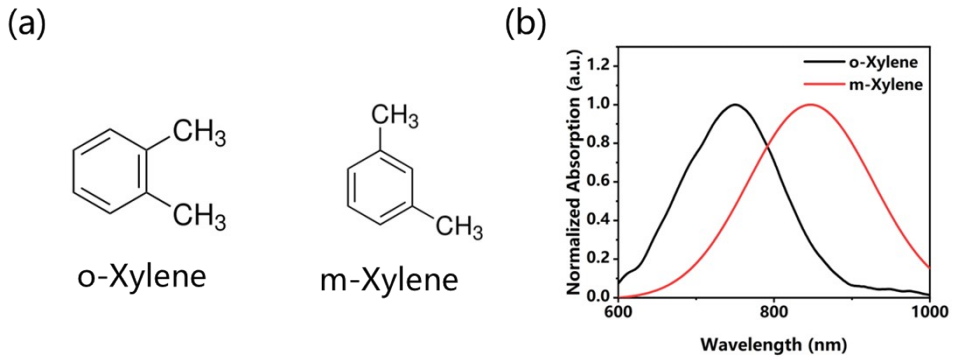

Figure S17. (a) the chemical structure and (b)the UV-Vis spectra for Reichardt's Dye in o-Xylene and m-Xylene.

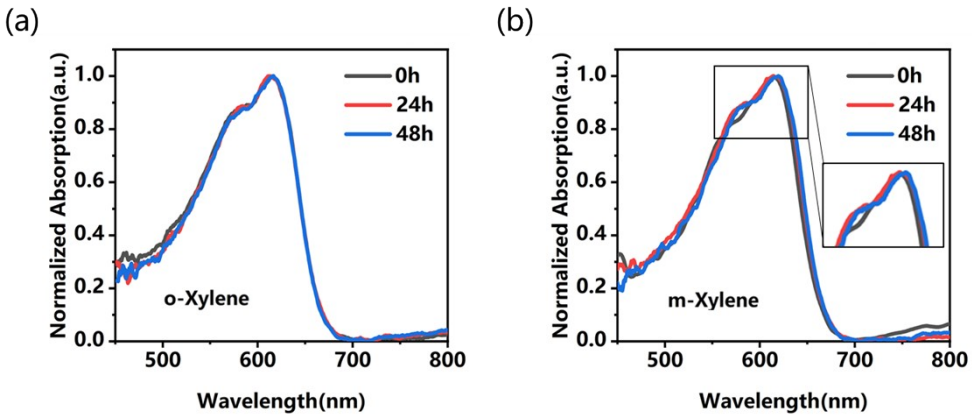

Figure S18. (a) The UV-vis absorption spectra of the PM6 solutions in different aging time using o-Xylene and m-Xylene as the solvents.

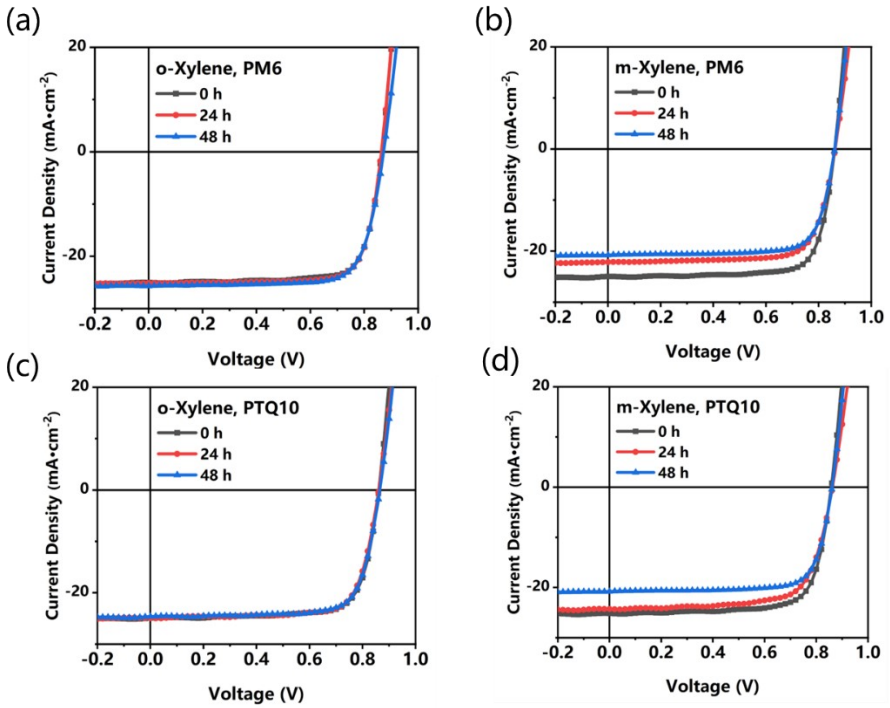

Figure S19. *J-V* curves of PM6/L8-BO and PTQ10/L8-BO OSCs using o-Xylene and m-Xylene as the solvent of doner solutions with different aging times.

Table S1. The viscosities of solutions measured under different conditions.

Aging time	Toluene			TMB		
	3 mg mL^{-1}	5 mg mL^{-1}	7 mg mL^{-1}	3 mg mL^{-1}	5 mg mL^{-1}	7 mg mL^{-1}
0 h	1.998[a]	18.448	36.894	2.306	4.612	7.840
24 h	2.036	20.464	79.342	2.332	4.602	7.852
48 h	2.002	21.126	98.572	2.328	4.618	7.858

[a]The unit for all the data is mm^2 s^{-1}

Table S2. D-spacing and crystalline coherent length (CCL) quantified based on the GIWAXS image of PM6 films.

Condition	*(010)* in plane		*(010)* out of plane		*(100)* in plane		*(100)* out of plane	
	D-spacing/Å	CCL/nm	D-spacing/Å	CCL/nm	D-spacing/Å	CCL/nm	D-spacing/Å	CCL/nm
Toluene, 0 h	3.756	3.30	3.767	3.02	22.832	58.34	19.382	72.46
Toluene, 48 h	3.753	4.27	3.779	2.12	23.034	57.09	19.623	74.36
TMB, 0 h	3.775	3.58	3.779	3.21	22.631	57.67	19.382	79.60
TMB, 48 h	3.773	3.48	3.778	3.18	22.875	57.89	19.443	78.84

Table S3. The paracrystallinity of PM6 films prepared by Toluene/TMB-based

solutions.

Condition	*(010)* in plane			*(010)* out of plane		
	D-spacing (Å)	CCL (nm)	g (%)	D-spacing (Å)	CCL (nm)	g (%)
Toluene, 0 h	3.756	3.30	13.46	3.767	3.02	14.09
Toluene, 48 h	3.753	4.27	11.83	3.779	2.12	16.85
TMB, 0 h	3.775	3.58	12.96	3.779	3.21	13.69
TMB, 48 h	3.773	3.48	13.14	3.778	3.18	13.75

Table S4. The carrier mobilities of PM6/L8-BO OSCs.

Aging time	Toluene		TMB	
	μ_h (cm^{-2} V^{-1} s^{-1})	μ_e (cm^{-2} V^{-1} s^{-1})	μ_h (cm^{-2} V^{-1} s^{-1})	μ_e (cm^{-2} V^{-1} s^{-1})[a]
0 h	（2.67±0.18）$\times 10^{-4}$	（3.31±0.21）$\times 10^{-4}$	（2.66±0.20）$\times 10^{-4}$	（3.12±0.22）$\times 10^{-4}$
24 h	（2.12±0.29）$\times 10^{-4}$	（2.73±0.34）$\times 10^{-4}$	（2.71±0.24）$\times 10^{-4}$	（3.03±0.24）$\times 10^{-4}$
48 h	（1.79±0.35）$\times 10^{-4}$	（2.45±0.44）$\times 10^{-4}$	（2.62±0.21）$\times 10^{-4}$	（3.14±0.20）$\times 10^{-4}$

[a] The average mobilities are obtained from 10 devices.

Table S5. The D-spacing and CCL extracted from the one-dimensional data of

GIWAXS for blend films.

condition	*(010)* out of plane		L8-BO *(100)* in plane		PM6 *(100)* in plane	
	D-spacing (Å)	CCL (nm)	D-spacing (Å)	CCL (nm)	D-spacing (Å)	CCL (nm)
Toluene, 0 h	3.558	21.36	17.493	125.83	21.021	92.35
Toluene, 48 h	3.489	24.15	17.432	138.54	21.132	89.71
TMB, 0 h	3.562	21.21	17.904	119.22	21.255	91.62
TMB, 48 h	3.768	21.11	17.556	121.38	20.933	91.01

Table S6. The specific photovoltaic parameters of PM6/L8-BO OSCs prepared by 3 mg mL^{-1} Toluene-based PM6 solutions with different aging times.

Aging time	V_{OC} (V)	J_{SC} (mA cm^{-2})	FF (%)	PCE (%)[a]
0 h	0.860	25.54	75.65	16.42± 0.18 (16.61)[b]
24 h	0.858	25.51	74.62	16.38 ± 0.22 (16.54)
48 h	0.855	25.67	73.83	16.19 ± 0.27 (16.43)
1 wk	0.848	24.81	71.18	15.22 ± 0.41 (15.52)
1 m	0.847	24.43	69.67	14.31 ± 0.63 (14.92)
2 m	0.845	23.91	68.14	13.89 ± 0.55 (14.47)

[a] The average PCEs are obtained from 10 devices.

[b] The maximum value of PCE is shown in the bracket.

Table S7. The specific photovoltaic parameters of PM6/L8-BO OSCs prepared by 3 mg

mL^{-1} TMB-based PM6 solutions with different aging times.

Aging time	V_{OC} (V)	J_{SC} (mA cm^{-2})	FF (%)	PCE (%)[a]
0 h	0.861	25.43	75.33	16.47± 0.19 (16.60)[b]
24 h	0.858	25.51	75.38	16.42 ± 0.21 (16.67)
48 h	0.857	25.65	75.11	16.50 ± 0.23 (16.72)
1 wk	0.861	25.55	75.23	16.49 ± 0.15 (16.63)
1 m	0.856	25.71	74.78	16.45 ± 0.24 (16.58)
2 m	0.858	25.61	74.90	16.45 ± 0.17 (16.57)

[a] The average PCEs are obtained from 10 devices.

[b] The maximum value of PCE is shown in the bracket.

Table S8. The specific photovoltaic parameters of PM6/L8-BO:BTP-ec9 OSCs with different aging times using Toluene/TMB-based PM6 solutions.

Condition	V_{OC} (V)	J_{SC} (mA cm^{-2})	FF (%)	PCE (%)[a]
Toluene, 0 h	0.868	26.57	77.61	17.87 ± 0.14 (18.04)[b]
Toluene, 24 h	0.867	25.88	74.98	16.82 ± 0.35 (17.34)
Toluene, 48 h	0.865	25.32	72.94	15.77 ± 0.68 (16.32)
TMB, 0 h	0.870	26.49	77.73	17.92 ± 0.15 (18.01)
TMB, 24 h	0.869	26.46	77.78	17.89 ± 0.23 (17.98)
TMB, 48 h	0.872	26.42	77.71	17.91 ± 0.21 (18.02)

[a] The average PCEs are obtained from 10 devices.

[b] The maximum value of PCE is shown in the bracket.

Table S9. The specific photovoltaic parameters of PTQ10/L8-BO OSCs with different

aging times using Toluene/TMB-based PTQ10 solutions.

Condition	V_{OC} (V)	J_{SC} (mA cm^{-2})	FF (%)	PCE (%)[a]
Toluene, 0 h	0.853	25.77	74.25	16.31 ± 0.23 (16.62)[b]
Toluene, 24 h	0.850	24.93	70.56	14.96 ± 0.39 (15.48)
Toluene, 48 h	0.850	24.34	69.12	14.28 ± 0.51 (14.91)
TMB, 0 h	0.854	25.64	74.28	16.28 ± 0.19 (16.48)
TMB, 24 h	0.856	25.58	74.51	16.30 ± 0.24 (16.53)
TMB, 48 h	0.853	25.76	74.11	16.28 ± 0.17 (16.51)

[a] The average PCEs are obtained from 10 devices.

[b] The maximum value of PCE is shown in the bracket.

Table S10. The specific photovoltaic parameters of PCE10/L8-BO OSCs with different aging times using Toluene/TMB-based PCE10 solutions.

Condition	V_{OC} (V)	J_{SC} (mA cm^{-2})	FF (%)	PCE (%)[a]
Toluene, 0 h	0.721	21.15	71.41	10.82 ± 0.23 (11.32)[b]
Toluene, 24 h	0.721	20.82	70.20	10.58± 0.39 (11.28)
Toluene, 48 h	0.716	20.76	68.92	10.26 ± 0.51 (10.74)
TMB, 0 h	0.720	21.24	71.68	10.94 ± 0.19 (11.19)
TMB, 24 h	0.722	21.31	70.02	10.78± 0.24 (11.08)
TMB, 48 h	0.722	21.18	70.66	10.83 ± 0.23 (11.24)

[a] The average PCEs are obtained from 10 devices.

[b] The maximum value of PCE is shown in the bracket.

Table S11. The specific photovoltaic parameters of PM6/L8-BO OSCs with different

aging times using o-Xylene/m-Xylene-based PM6 solutions.

Condition	V_{OC} (V)	J_{SC} (mA cm^{-2})	FF (%)	PCE (%)[a]
o-Xylene, 0 h	0.865	25.45	77.24	16.91 ± 0.14 (17.09)[b]
o-Xylene, 24 h	0.866	25.41	77.29	16.87 ± 0.15 (17.05)
o-Xylene, 48 h	0.866	25.32	77.17	16.85 ± 0.18 (17.06)
m-Xylene, 0 h	0.863	25.26	77.48	16.94 ± 0.15 (17.05)
m-Xylene, 24 h	0.865	23.84	75.68	15.57 ± 0.38 (16.04)
o-Xylene, 48 h	0.864	23.26	74.55	14.98 ± 0.44 (15.62)

[a] The average PCEs are obtained from 10 devices.

[b] The maximum value of PCE is shown in the bracket.

Table S12. The specific photovoltaic parameters of PTQ10/L8-BO OSCs with different aging times using o-Xylene/m-Xylene-based PTQ10 solutions.

Condition	V_{OC} (V)	J_{SC} (mA cm^{-2})	FF (%)	PCE (%)[a]
o-Xylene, 0 h	0.858	24.83	75.88	16.23 ± 0.14 (16.39)[b]
o-Xylene, 24 h	0.861	24.67	75.94	16.13 ± 0.17 (16.36)
o-Xylene, 48 h	0.857	24.71	75.97	16.08 ± 0.18 (16.28)
m-Xylene, 0 h	0.856	25.12	75.74	16.28 ± 0.18 (16.43)
m-Xylene, 24 h	0.858	24.36	74.83	15.78 ± 0.23 (16.06)
m-Xylene, 48 h	0.855	20.86	76.56	13.73± 0.46 (14.24)

[a] The average PCEs are obtained from 10 devices.

[b] The maximum value of PCE is shown in the bracket.

References

1 J. Xue, H. Zhao, B. Lin, Y. Wang, Q. Zhu, G. Lu, B. Wu, Z. Bi, X. Zhou, C. Zhao, G. Lu, K. Zhou, W. Ma, *Adv. Mater*., 2022, **34**, 2202659.

2 J.-D. Chai, M. Head-Gordon, *Chem. Phys*., 2008, **10,** 6615.

3 W. J. Hehre, R. Ditchfield, J. A. Pople, *J. Chem. Phys*., 1972, **56**, 2257–2261.

4 P. C. Hariharan, J. A. Pople, Theor. *Chim. Acta*, 1973, **28**, 213–222.

5 W. R. Wadt, P. J. Hay, *J. Chem. Phys*., 1985, **82**, 284.

6 Gaussian 16, Revision A.03, M. J. Frisch, G. W. Trucks, H. B. Schlegel, G. E. Scuseria, M. A. Robb, J. R. Cheeseman, G. Scalmani, V. Barone, G. A. Petersson, H. Nakatsuji, X. Li, M. Caricato, A. V. Marenich, J. Bloino, B. G. Janesko, R. Gomperts, B. Mennucci, H. P. Hratchian, J. V. Ortiz, A. F. Izmaylov, J. L. Sonnenberg, D. Williams-Young, F. Ding, F. Lipparini, F. Egidi, J. Goings, B. Peng, A. Petrone, T. Henderson, D. Ranasinghe, V. G. Zakrzewski, J. Gao, N. Rega, G. Zheng, W. Liang, M. Hada, M. Ehara, K. Toyota, R. Fukuda, J. Hasegawa, M. Ishida, T. Nakajima, Y. Honda, O. Kitao, H. Nakai, T. Vreven, K. Throssell, J. A. Montgomery, Jr., J. E. Peralta, F. Ogliaro, M. J. Bearpark, J. J. Heyd, E. N. Brothers, K. N. Kudin, V. N. Staroverov, T. A. Keith, R. Kobayashi, J. Normand, K. Raghavachari, A. P. Rendell, J. C. Burant, S. S. Iyengar, J. Tomasi, M. Cossi, J. M. Millam, M. Klene, C. Adamo, R. Cammi, J. W. Ochterski, R. L. Martin, K. Morokuma, O. Farkas, J. B. Foresman, and D. J. Fox, Gaussian, Inc., Wallingford CT, 2016.

7 T. Lu, Q. Chen, *J. Phys. Chem. A*, 2023, **127**, 7023−7035.

8 T. Lu, F. W. Chen. *J. Comput. Chem*., 2012, **33**, 580.

9 G. Kresse, J. Furthmuller, *Phys. Rev. B*, 1996, **54,** 11169-11186.

10 J. P. Perdew, K. Burke, M. Ernzerhof, *Phys. Rev. Lett*., 1996, **77**, 3865-3868.

11 P. E. Blochl, *Phys. Rev. B*, 1994, **50**, 17953-17979.

12 S. Grimme, *J. Comput. Chem*., 2006, **27**, 1787-1799.

13 M. Parrinello, A. Rahman, *Phys. Rev. Lett*., 1980, **45**, 1196-1199.

14 Y. Zheng, Z. Yao, T. Lei, J. Dou, C. Yang, L. Zou, X. Meng, W. Ma, J. Wang, J. Pei, *Adv. Mater*., 2017, **29**, 1701072.

15 A. Hexemer, W. Bras, J. Glossinger, E. Schaible, E. Gann, R. Kirian, A. MacDowell, M. Church, B. Rude, H. Padmore, *J. Phys. Conf. Ser*., 2010, **247**, 012007.

16 F. S. Shirazi, B. Hemmateenejad, A. M. Mehranpourb, *Anal. Methods*, 2013, **5**, 891-896.

17 X. Jiao, L. Ye, H. Ade, *Adv. Energy Mater*., 2017, **7**, 1700084.